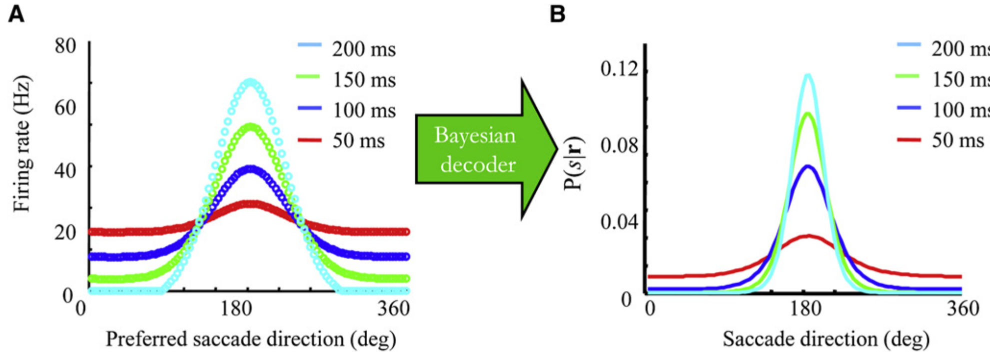

Figure 4. Continuous Decision Making (as Illustrated in Figure 1B)

(A) Firing rates of model neurons in LIP at four different times for a coherence of 51.2%. The direction of the moving dots is 180°.

(B) Probability distributions encoded by the firing rates shown in (A) averaged over 1000 trials. As expected, the peak of the distribution is close to 180° and the variance of the distribution decreases over time.

in the LIP layer of the model as a function of coherence and number of choices is similar to what has been reported in vivo (see Figure 7).

Experimental Predictions

Our model makes two experimentally testable predictions. The first is that the population response in LIP encodes a probability distribution over the stimulus and, more importantly, that this distribution reflects both the reliability of the evidence and the performance of the animal. Therefore, we predict that if the population activity in LIP is decoded with the same method used in our simulations, the results will match those shown in Figures 3A and 3B and Figure 5A. Rigorously testing this prediction requires multiunit recordings in LIP, which are not currently available. However, we can test it qualitatively with the spike trains obtained from single cell recordings (Roitman and Shadlen, 2002). If the spikes trains in LIP reflect the quality of the sensory data, the expected log odds computed from these spike trains should grow linearly with time, and the rate of growth should be proportional to coherence. We have performed this analysis, and this is indeed what we found, as illustrated in Figure 3D. Furthermore, if these odds reflect the performance of the animal, we should find that the log odds in LIP at decision time grows with coherence for both the two- and four-choice experiment (since performance improves with coherence). Again, this is what we observed (Figure 5B).

Recent experiments suggest that a similar property may hold for buildup cells in the superior colliculus (Kim and Basso, 2008; Ratcliff et al., 2006). For instance, Kim and Basso (2008) have recorded simultaneously from neurons responding to the selected

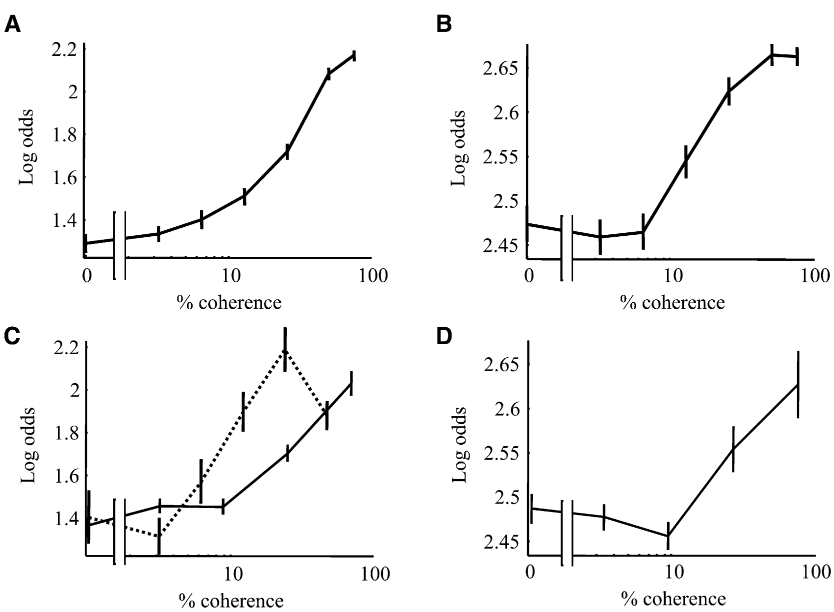

Figure 5. Average Log Odds at Decision Time Computed from the Model and Data for the Two- and Four-Choice Experiments

(A) Average log odds at decision time for a two-choice experiment estimated from two neurons in the LIP layer of the model tuned to 0° and 180° on trials for which the model selected 180°. The average log odds is defined as the log of the ratio of the probability that the direction is equal to 180° to the probability that it is equal to 0° averaged over trials.

(B) Same as in (A) but for the four-choice experiment (for consistency with the two-choice experiment, we use log odds in the four-choice experiment).

(C) Same as in (A) but for actual LIP neurons (n = 45) in the two-choice experiment (dotted line, data from Roitman and Shadlen, 2002; solid line, data from Churchland et al., 2008).

(D) Same as in (B) but for actual LIP neurons (n = 51–70) in the four-choice experiment (data from Churchland et al., 2008). In both (C) and (D), the log odds increases with coherence. Since higher coherence also implies higher performance, log odds also increases with performance. This is indeed what is expected if the posterior encoded in LIP reflects the quality of the data and, at decision time, the performance of the animal. On these plots, the y axis is arbitrary up to a multiplicative factor.

The method used to obtain the error bars is described in the Supplemental Data.